Digital Signal Processing 65 (2017) 1–10

Contents lists available at ScienceDirect

Digital Signal Processing

www.elsevier.com/locate/dsp

Angle and mutual coupling estimation in bistatic MIMO radar based on PARAFAC decomposition

Fangqing Wen [a,*], Xiaodong Xiong [a], Zijing Zhang [b]

[a] Electronic and Information School, Yangtze University, Jingzhou, 434023, China
[b] National Laboratory of Radar Signal Processing, Xidian University, Xi'an, 710071, China

ARTICLE INFO

Article history:
Available online 3 March 2017

Keywords:
Bistatic MIMO radar
Angle estimation
Mutual coupling
PARAFAC decomposition

ABSTRACT

In this paper, a PARAFAC decomposition-based algorithm is developed for joint direction-of-departure and direction-of-arrival estimation in the presence of unknown mutual coupling for bistatic multiple-input multiple-output radar. A three-order tensor is formulated which links the estimations of coupled direction matrices to the PARAFAC model. The coupling effects of the direction matrices are compensated by two selective matrices, and the angles are obtained from the estimated direction matrices. Then the mutual coupling coefficients of the transmitter and the receiver are estimated using the subspace method. Unlike existing algorithms, PARAFAC decomposition before decoupling operation results in more accurate angle estimation, which brings better mutual coupling coefficients estimation than the ESPRIT-Like and unitary HOSVD methods. The proposed algorithm does not require spectral peak searching or eigenvalue decomposition of the received signal covariance matrix, and it can achieve automatic pairing of the estimated angles. The identifiability and computation complexity of the presented algorithm are analysed and Cramer–Rao bounds of joint angle and mutual coupling estimation are derived. Numerical experiments verify the effectiveness and improvement of our algorithm.

1. Introduction

Multiple-input multiple-output (MIMO) radar is a novel radar system that has aroused extensive attention [1,2]. The concept of MIMO radar is that the radar systems simultaneously transmit mutually orthogonal waveforms with multiple antennas and receive the reflected echoes with multiple antennas. The information of an individual transmitter-to-receiver path is separated by matched filters at the receiving end. The virtual transmitter-to-receiver paths enable MIMO radar to achieve more degrees of freedom than the traditional phase-array radar [3]. Theoretical research indicates that MIMO radar has several built-in advantages in suppressing noise, overcoming fading effect, improving spatial resolution, enhancing parameter identifiability, etc. [4–6]. In terms of the antennas configuration, MIMO radar can be divided into two classes. One is statistical MIMO radar [7], which takes advantage of widely separated antennas to achieve spatial diversity to solve target scintillation problem. The other one is collocated MIMO radar [8], whose antennas are closely placed in both transmit array and receive array to obtain unambiguous angle estimation. In this paper, we mainly concentrate on the parameter estimation problem of collocated MIMO radar.

Direction-of-departure (DOD) and direction-of-arrival (DOA) estimation is a canonical problem in bistatic MIMO radar that has received intensive attention in the last decade. In [9] and [10], Capon and multiple signal classification (MUSIC) algorithms were introduced into angle estimation for MIMO radar, which estimate parameters via spectral peak searching and suffer from high computational complexity. ESPRIT method, which is short for the estimation method of signal parameters via rotational invariance techniques, has been discussed in [11]. It utilizes the shift invariance property of the virtual array in MIMO radar for parameters estimation, and ESPRIT method does not require spectral peak searching. To reduce the computation load, the unitary transform based ESPRIT algorithm was proposed in [12], which computes ESPRIT with real number and has estimation performance close to that of the ESPRIT method. Nevertheless, the above algorithms ignore the inherent multidimensional structure in the received data. Signal processing tools based on multilinear tensor algebra play a role in promoting parameters estimation performance [13,14]. In [15,16] and [17,18], separately, higher-order singular value decomposition (HOSVD) algorithm and parallel factor analysis (PARAFAC) method were presented, which turned out to be effective in angle estimation for MIMO radar.

* Corresponding author.
E-mail address: wfqltt@163.com (F. Wen).

http://dx.doi.org/10.1016/j.dsp.2017.02.011
1051-2004/

In the presence of unknown mutual coupling, the accuracy of angle estimation in [9–12,15–18] will be degraded remarkably. The mutual coupling problem in radar system has been investigated in [19–21]. The MUSIC-Like scheme was developed in [19], which performs twice one-dimensional peak searches to obtain the estimates of the angles. The ESPRIT-Like approach was introduced in [20], in contrast to MUSIC-Like algorithm, it requires no peak searching. Taking the multidimensional structure of the received data into consideration, the unitary HOSVD method was derived by incorporating the forward-backward averaging techniques [21], which is applicable to coherent sources. However, the drawback of this approach is the reduction of effective array aperture size, resulting in lower resolution and accuracy. Furthermore, the decoupling operation before SVD or multi-SVD implies that only a part of array is utilized for angle estimation. The data from the first and last few elements is omitted in the mentioned algorithms, and in general this will result in performance degradation compared to other methods based on the whole array. In addition, a common drawback that the existing algorithms share is that additional pairing is required, thus leading to extra computation load.

Motivated by the above shortcomings, we present a PARAFAC decomposition based algorithm for joint DOD and DOA estimation with unknown mutual coupling in this paper, which can be be viewed as an extension of the approach in [17]. By stacking the received data into a third-order tensor, the multidimensional structure inherent in received data are fully utilized. The PARAFAC decomposition is employed to obtain the coupled direction matrices, which makes full use of all the antenna elements. Furthermore, the selective matrices are applied for decoupling, then the proposed algorithm obtain automatically paired estimations of DOD and DOA. Thereafter, the mutual coupling coefficients are easily estimated using subspace method. As the decoupling operation is carried out after signal decomposition, more robust and accurate direction matrices will be obtained in the proposed algorithm. Therefore, the proposed method provides better angle estimation performance than both ESPRIT-Like algorithm [20] and unitary HOSVD method [21]. In addition, the formulas of Cramer–Rao bounds (CRB) for angle and mutual coupling estimation are derived. Simulation results are given to illustrate the effectiveness of the proposed algorithm.

The paper outline is as follows. The data model for the bistatic MIMO radar is presented in section 2. The PARAFAC decomposition algorithm is derived in section 3. The performance and complexity of the proposed algorithm is discussed in section 4. Simulation results are given in section 5. We end the paper by a brief conclusion in section 6.

Notation: capital letter $\mathbf{X}$ and lower case $\mathbf{x}$ in bold denote matrices and vectors, respectively. The $M \times M$ identity matrix is denoted by $\mathbf{I}_M$, and the $M \times M$ inverse permutation matrix is denoted by $\mathbf{\Pi}_M$. The superscript $(\mathbf{X})^T$, $(\mathbf{X})^H$, $(\mathbf{X})^{-1}$ and $(\mathbf{X})^\dagger$ represent the operations of transpose, Hermitian transpose, inverse and pseudo-inverse, respectively; The subscript $\|\mathbf{X}\|_F$ denotes the Frobenius norm of $\mathbf{X}$; $\otimes$ stands for the Kronecker product; The Khatri–Rao product (column-wise Kronecker product) is denoted by $\odot$, i.e., $[\mathbf{a}_1, \mathbf{a}_2, \cdots, \mathbf{a}_K] \odot [\mathbf{b}_1, \mathbf{b}_2, \cdots, \mathbf{b}_K] = [\mathbf{a}_1 \otimes \mathbf{b}_1, \mathbf{a}_2 \otimes \mathbf{b}_2, \cdots, \mathbf{a}_K \otimes \mathbf{b}_K]$; Toeplitz[$\mathbf{r}$] denotes the symmetric Toeplitz matrix constructed by the vector $\mathbf{r}$; diag($\mathbf{r}$) denotes the diagonalization operation. blkdiag$\{\mathbf{v}_1, \cdots, \mathbf{v}_L\}$ denotes a block-diagonal matrix with $\mathbf{r}_1, \cdots, \mathbf{r}_L$ being its diagonal sub-matrices. Some preliminaries including basic definitions of tensor and PARAFAC decomposition are given in the appendix.

2. Signal model

Consider a bistatic MIMO radar system equipped with an M-element transmit array and an N-element receive array, both of which are omni-directional uniform linear arrays (ULA) with half-wavelength spacing. Neither gain-phase error nor position error is considered in this paper. Assume that K non-coherent point targets appear in the far-field of the antennas, and all the targets are in the same range bin of interest, otherwise they can be resolved in range. The DOD and the DOA for the k-th target are denoted by φ_k and θ_k, respectively. Additional assumptions are that the transmit antennas emit orthogonal narrowband waveforms with the same carrier frequency. The echoes are collected by the receive antenna array and are detected by a set of matched filters. The noiseless output of the matched filters in the n-th receive antenna takes the form

$$\mathbf{r}_n(t) = \sum_{k=1}^{K} \bar{\mathbf{a}}_t(\varphi_k)\, \bar{a}_r^n(\theta_k)\, s_k(t) \tag{1}$$

where $\bar{\mathbf{a}}_t(\varphi_k) = \left[\bar{a}_t^1(\varphi_k), \cdots, \bar{a}_t^M(\varphi_k)\right]^T \in \mathbb{C}^{M\times 1}$ and $\bar{\mathbf{a}}_r(\theta_k) = \left[\bar{a}_r^1(\theta_k), \cdots, \bar{a}_r^N(\theta_k)\right]^T \in \mathbb{C}^{N\times 1}$ respectively denote the receive steering vector and the transmit steering vector for the k-th target, with the column element $\bar{a}_r^n(\theta_k) = \exp\{-j\pi(n-1)sin\theta_k\}$, $(n = 1, 2, \cdots, N)$, and $\bar{a}_t^m(\varphi_k) = \exp\{-j\pi(m-1)\sin\varphi_k\}$, $(m = 1, 2, \cdots, M)$. The waveform $s_k(t) = \alpha_k \exp\{j2\pi f_k t/f_s\}$ is the product of the radar cross section (RCS) α_k and the Doppler frequency shift f_k/f_s of the k-th target, with f_k bing the Doppler frequency, f_s being the pulse repeat frequency. Arrange the receive waveforms as $\bar{\mathbf{x}}(t) = [\mathbf{r}_1(t), \cdots, \mathbf{r}_N(t)]^T$, we have

$$\bar{\mathbf{x}}(t) = \left[\bar{\mathbf{a}}_r(\theta_1) \otimes \bar{\mathbf{a}}_t(\varphi_1), \cdots, \bar{\mathbf{a}}_r(\theta_K) \otimes \bar{\mathbf{a}}_t(\varphi_K)\right]\mathbf{s}(t) \tag{2}$$

where $\mathbf{s}(t) = [\mathbf{s}_1(t), \cdots, \mathbf{s}_K(t)]^T$ is a column vector. Let the transmit direction matrix $\bar{\mathbf{A}}_T = [\bar{\mathbf{a}}_t(\varphi_1), \cdots, \bar{\mathbf{a}}_t(\varphi_K)] \in \mathbb{C}^{M\times K}$, the receive direction matrix $\bar{\mathbf{A}}_R = [\bar{\mathbf{a}}_r(\theta_1), \cdots, \bar{\mathbf{a}}_r(\theta_K)] \in \mathbb{C}^{N\times K}$. Suppose the RCS of all targets fulfill the Swerling I model, after collecting a total of L snapshots, the received data becomes $\bar{\mathbf{X}} = [\bar{\mathbf{x}}(1), \cdots, \bar{\mathbf{x}}(L)] \in \mathbb{C}^{MN\times L}$, which can be formulated as

$$\bar{\mathbf{X}} = \left[\bar{\mathbf{A}}_R \odot \bar{\mathbf{A}}_T\right]\mathbf{S}^T = \bar{\mathbf{A}}\mathbf{S}^T \tag{3}$$

where $\mathbf{S} = [\mathbf{s}_1, \cdots, \mathbf{s}_L]^T$ is a $L \times K$ coefficient matrix with the l-th $(l = 1, \ldots, L)$ row vector $\mathbf{s}_l = [s_1(lT), \cdots, s_K(lT)]^T \in \mathbb{C}^{K\times 1}$, T is the pulse recurrence period. Here the direction matrix $\bar{\mathbf{A}} = [\bar{\mathbf{a}}(\theta_1, \varphi_1), \cdots, \bar{\mathbf{a}}(\theta_K, \varphi_K)] \in \mathbb{C}^{MN\times K}$, with the k-th $(k = 1, 2, \cdots, K)$ column $\bar{\mathbf{a}}(\theta_k, \varphi_k) = \bar{\mathbf{a}}_r(\theta_k) \otimes \bar{\mathbf{a}}_t(\varphi_k)$, which is known as the virtual array steering vector.

In the presence of mutual coupling in both transmit array and receive array, the receive signal model in Eq. (3) will be changed. The magnitude of mutual coupling between two neighboring elements of the ULA will be the same, while mutual coupling coefficients between two elements that are far enough from each other can often be approximated as zeros. Suppose there are $P+1$ nonzero mutual coupling coefficients in both transmit and receive arrays with $\min\{M, N\} > 2P$. The mutual coupling matrices of the transmit array $\mathbf{C}_T$ and receive array $\mathbf{C}_R$ can be modeled as banded symmetric Toeplitz matrices [19–21]

$$\begin{cases} \mathbf{C}_T = \text{toeplitz}[\mathbf{c}_t, 0, \cdots 0] \\ \mathbf{C}_R = \text{toeplitz}[\mathbf{c}_r, 0, \cdots 0] \end{cases} \tag{4}$$

where $\mathbf{c}_t = [c_{t0}, \cdots, c_{tP}]$ and $\mathbf{c}_r = [c_{r0}, \cdots, c_{rP}]$ denote the $P+1$ nonzero mutual coupling coefficients with $0 < |c_{tP}| < \cdots |c_{t1}| < c_{t0} = 1$ and $0 < |c_{rP}| < \cdots < |c_{r1}| < c_{r0} = 1$, respectively. Taking the noise into consideration, the output of the radar system with mutual coupling effect can be expressed in matrix form [20,21]

$$\mathbf{X} = \left[\left(\mathbf{C}_R\bar{\mathbf{A}}_R\right) \odot \left(\mathbf{C}_T\bar{\mathbf{A}}_T\right)\right]\mathbf{S}^T + \mathbf{W}_S = \mathbf{A}\mathbf{S}^T + \mathbf{W}_S \tag{5}$$

where $\mathbf{A} = \mathbf{A}_R \odot \mathbf{A}_T = [\mathbf{a}(\theta_1, \varphi_1), \cdots, \mathbf{a}(\theta_K, \varphi_K)] \in \mathbb{C}^{MN\times K}$ is the coupled visual direction matrix. $\mathbf{A}_R = \mathbf{C}_R\bar{\mathbf{A}}_R = [\mathbf{a}_r(\theta_1), \cdots, \mathbf{a}_r(\theta_K)]$

denotes the coupled received direction matrix, and $\mathbf{A}_T = \mathbf{C}_T\bar{\mathbf{A}}_T = [\mathbf{a}_t(\varphi_1), \cdots, \mathbf{a}_t(\varphi_K)]$ stands for the coupled transmit direction matrix. $\mathbf{W}_S \in \mathbb{C}^{MN\times L}$ is assumed to be independent, zero-mean complex Gaussian noise.

Remark 1. It is assumed in this paper that the number of mutual coupling coefficients is known as a prior condition. Mutual coupling uncertainties should be considered as the gain-phase error model [22], which is the topic of current work [23,24], but beyond the scope of this paper.

By implementing the PARAFAC decomposition model in Definition 3, the received data in Eq. (5) can be denoted as a three-order tensor as well

$$\mathcal{X}(m,n,l) = \sum_{k=1}^{K} \mathbf{A}_T(m,k)\,\mathbf{A}_R(n,k)\,\mathbf{S}(l,k) + \mathcal{W}(m,n,l) \quad (m=1,\ldots,M;\, n=1,\ldots,N;\, l=1,\ldots,L) \tag{6}$$

where $\mathcal{X}(m,n,l)$ denotes the (m,n,l)-th element of the three-order tensor $\mathcal{X}$. $\mathbf{A}_T(n,k)$ represents the (n,k)-th element of $\mathbf{A}_T$ and is similar to others. $\mathcal{W}(m,n,l)$ is the rearranged noise measurement. Generally speaking, Eq. (5) is the matricized version of a PARAFAC decomposition model, and the rearranged data in Eq. (6) can be viewed as the tensor form of a PARAFAC decomposition model. Indeed, the different forms of a PARAFAC decomposition model are equivalent. According to Definition 2, the expression in Eq. (5) can be regarded as transpose of the 3-mode matrix unfolding of $\mathcal{X}$, i.e., $\mathbf{X} = \mathcal{X}_{(3)}^T$, which can be interpreted as the slices of the three dimensional data along the spatial direction. The symmetry of the trilinear model in Eq. (6) allows two more matrix system rearrangements. The 1-mode matrix unfolding of $\mathcal{X}$ can be constructed as follows

$$\mathbf{Y} = \mathcal{X}_{(1)}^T = [\mathbf{S}\odot\mathbf{A}_R]\,\mathbf{A}_T^T + \mathbf{W}_T \tag{7}$$

where $\mathbf{W}_T$ denotes the rearranged noise slices along the transmit array direction. Eq. (7) can be interpreted as the slices of the three dimensional data along the transmit array direction. Similarly, the 2-mode matrix unfolding of $\mathcal{X}$ can be constructed as follows

$$\mathbf{Z} = \mathcal{X}_{(2)}^T = [\mathbf{A}_T\odot\mathbf{S}]\,\mathbf{A}_R^T + \mathbf{W}_R \tag{8}$$

where $\mathbf{W}_R$ denotes the rearranged noise slices along the receive array direction. Eq. (8) can be interpreted as the slices of the three dimensional data along the receive array direction.

3. Joint angle and mutual coupling estimation

3.1. Coupled direction matrix estimation

Trilinear alternating least square (TALS) is an effective algorithm to solve the PARAFAC decomposition problem. The essence of TALS can be described as the following steps: (**a**) Fitting one of the slicing matrices **X**, **Y** or **Z** using least squares (LS) method, where the remaining two matrices are previously obtained, (**b**) Fitting the other two matrices in a similar way, and (**c**) Repeat (a) and (b) until the stop conditions is satisfied. The details of solving the above PARAFAC model with TALS algorithm is described as follows.

According to Eq. (5), the LS fitting of **X** is

$$f_{\mathbf{X}} = \min_{\mathbf{A}_R,\mathbf{A}_T,\mathbf{S}} \left\|\mathbf{X} - [\mathbf{A}_R\odot\mathbf{A}_T]\,\mathbf{S}^T\right\|_F \tag{9}$$

Therefore, the LS estimate of **S** is

$$\hat{\mathbf{S}}^T = \left[\hat{\mathbf{A}}_R\odot\hat{\mathbf{A}}_T\right]^{\dagger}\mathbf{X} \tag{10}$$

with $\hat{\mathbf{A}}_R$ and $\hat{\mathbf{A}}_T$ denote the estimated $\mathbf{A}_R$ and $\mathbf{A}_T$ in the last iteration. With respect to Eq. (7), the LS fitting of **Y** is

$$f_{\mathbf{Y}} = \min_{\mathbf{S},\mathbf{A}_R,\mathbf{A}_T} \left\|\mathbf{Y} - [\mathbf{S}\odot\mathbf{A}_R]\,\mathbf{A}_T^T\right\|_F \tag{11}$$

The LS update for $\mathbf{A}_T$ is

$$\hat{\mathbf{A}}_T^T = \left[\hat{\mathbf{S}}\odot\hat{\mathbf{A}}_R\right]^{\dagger}\mathbf{Y} \tag{12}$$

where $\hat{\mathbf{S}}$ and $\hat{\mathbf{A}}_R$ are previously obtained **S** and $\mathbf{A}_R$. Similarly, according to Eq. (8), the LS fitting of **Z** is

$$f_{\mathbf{Z}} = \min_{\mathbf{A}_T,\mathbf{S},\mathbf{A}_R} \left\|\mathbf{Z} - [\mathbf{A}_T\odot\mathbf{S}]\,\mathbf{A}_R^T\right\|_F \tag{13}$$

and the LS update for $\mathbf{A}_R$ is

$$\hat{\mathbf{A}}_R^T = \left[\hat{\mathbf{A}}_T\odot\hat{\mathbf{S}}\right]^{\dagger}\mathbf{Z} \tag{14}$$

where $\hat{\mathbf{A}}_T$ and $\hat{\mathbf{S}}$ represent the previously estimated $\mathbf{A}_T$ and **S**, respectively. From Eq. (10), Eq. (12) and Eq. (14), one can see that matrices **S**, $\mathbf{A}_T$ and $\mathbf{A}_R$ are updated with conditioned LS, alternately. The iteration will repeat until algorithm convergence, indicating the restriction that $\epsilon = \left\|\mathbf{X} - \left[\hat{\mathbf{A}}_R\odot\hat{\mathbf{A}}_T\right]\hat{\mathbf{S}}^T\right\|_F^2 \le 10^{-8}$, or $\delta = \frac{|\epsilon_{\text{new}}-\epsilon_{\text{old}}|}{\epsilon_{\text{old}}} \le 10^{-10}$.

TALS algorithm is quite easy to implement and is guaranteed to converge. In TALS, the conditional update of any given matrix may either improve or maintain, but cannot worsen, the current fit. Global monotone convergence to (at least) a local minimum follows directly from this observation [25]. The number of sources K can be estimated with the approach proposed in [26]. If K is under- or over-estimated, the proposed method will invalid. The initialization matrices $\mathbf{A}_T$, $\mathbf{A}_R$ and **S** can be randomly generated or initialized by ESPRIT to speed up convergence, while it suffers from the occasional slowness of the convergence steps [27]. In order to avoid the brute force implementation of TALS in the raw data space, the COMFAC algorithm [28] is hereby adopted. In COMFAC algorithm, the high dimensional three-order tensor is first compressed into a smaller three-order tensor. Then the fitting operations are conducted in the condensed space, which only require a few TALS steps. Finally, the solutions are recovered to the original space.

3.2. DOD and DOA estimation

The uniqueness property under mild conditions is a key feature of PARAFAC decomposition. The identifiability of a PARAFAC model is described by the following theorem.

Theorem 1 *([29]). For any PARAFAC model constructed as Eq. (6), where* $\mathbf{A}_T \in \mathbb{C}^{M\times K}$, $\mathbf{A}_R \in \mathbb{C}^{N\times K}$, $\mathbf{S} \in \mathbb{C}^{L\times K}$. *Consider that all the matrices are full k-rank, if the parameter identifiability satisfies the inequality*

$$k_{\mathbf{A}_T} + k_{\mathbf{A}_R} + k_{\mathbf{S}} \ge 2K + 2 \tag{15}$$

then $\mathbf{A}_T$, $\mathbf{A}_R$ *and* **S** *are unique up to permutation and scaling of columns, where* $k_{\mathbf{A}_T}$, $k_{\mathbf{A}_R}$ *and* $k_{\mathbf{S}}$ *denote the k-rank of* $\mathbf{A}_T$, $\mathbf{A}_R$ *and* **S**, *respectively. The estimated matrices* $\hat{\mathbf{A}}_T$, $\hat{\mathbf{A}}_R$ *and* $\hat{\mathbf{S}}$ *satisfy* $\hat{\mathbf{A}}_T = \mathbf{A}_T\mathbf{\Pi}\mathbf{\Delta}_1 + \mathbf{N}_1$, $\hat{\mathbf{A}}_R = \mathbf{A}_R\mathbf{\Pi}\mathbf{\Delta}_2 + \mathbf{N}_2$ *and* $\hat{\mathbf{S}} = \mathbf{S}\mathbf{\Pi}\mathbf{\Delta}_3 + \mathbf{N}_3$, *where* $\mathbf{\Pi}$ *is a permutation matrix,* $\mathbf{N}_1$, $\mathbf{N}_2$ *and* $\mathbf{N}_3$ *represent the corresponding estimation error,* $\mathbf{\Delta}_1$ *and* $\mathbf{\Delta}_2$ *and* $\mathbf{\Delta}_3$ *stand for the diagonal scaling matrices satisfying* $\mathbf{\Delta}_1\mathbf{\Delta}_2\mathbf{\Delta}_3 = \mathbf{I}_K$. *It is worth noting that* $K < \min(\bar{M}, \bar{N})$ *is an inherent condition in the proposed algorithm. Otherwise the proposed algorithm will be invalid for large number of mutual coupling coefficients.*

Once TALS is accomplished, the estimated coupled direction matrices $\mathbf{A}_R$ and $\mathbf{A}_T$ can be obtained. To eliminate the mutual coupling effect, the following two selection matrices are utilized

$$\begin{cases} \mathbf{P}_R = \left[\mathbf{0}_{\bar{N}\times P}, \mathbf{I}_{\bar{N}}, \mathbf{0}_{\bar{N}\times P}\right] \in \mathbb{C}^{\bar{N}\times N} \\ \mathbf{P}_T = \left[\mathbf{0}_{\bar{M}\times P}, \mathbf{I}_{\bar{M}}, \mathbf{0}_{\bar{M}\times P}\right] \in \mathbb{C}^{\bar{M}\times M} \end{cases} \tag{16}$$

where $\bar{N} = N - 2P$ and $\bar{M} = M - 2P$. Multiplying the selection matrix to the left side of mutual coupling matrix yields

$$\mathbf{P}_R\mathbf{C}_R = \begin{bmatrix} c_{rP} & \cdots & c_{r0} & \cdots & c_{rP} & 0 & \cdots & 0 \\ 0 & c_{rP} & \cdots & c_{r0} & \cdots & c_{rP} & 0 & \cdots \\ 0 & \ddots & \ddots & \ddots & \ddots & \ddots & \ddots & 0 \\ 0 & \cdots & 0 & c_{rP} & \cdots & c_{r0} & \cdots & c_{rP} \end{bmatrix} \in \mathbb{C}^{\bar{N}\times N} \tag{17}$$

Here the m-th $(m = 2, \ldots, \bar{M})$ row in $\mathbf{P}_R\mathbf{C}_R$ is a circular shift of the $(m-1)$-th row. By multiplying $\mathbf{P}_R$ and $\mathbf{P}_T$ on the left sides of $\mathbf{A}_R$ and $\mathbf{A}_T$ we can get

$$\begin{cases} \mathbf{A}'_R = \mathbf{P}_R\mathbf{A}_R = \mathbf{P}_R\mathbf{C}_R\bar{\mathbf{A}}_R = \tilde{\mathbf{A}}_R\mathbf{D}_R \in \mathbb{C}^{\bar{N}\times K} \\ \mathbf{A}'_T = \mathbf{P}_T\mathbf{A}_T = \mathbf{P}_T\mathbf{C}_T\bar{\mathbf{A}}_T = \tilde{\mathbf{A}}_T\mathbf{D}_T \in \mathbb{C}^{\bar{M}\times K} \end{cases} \tag{18}$$

One can easily find that $\tilde{\mathbf{A}}_R$ and $\tilde{\mathbf{A}}_T$ are consist of the first $\bar{N}$ and $\bar{M}$ rows of $\bar{\mathbf{A}}_R$ and $\bar{\mathbf{A}}_T$, respectively. $\mathbf{D}_R = diag\left(d_r(\theta_1), \cdots, d_r(\theta_K)\right) \in \mathbb{C}^{K\times K}$ with the k-th diagonal element $d_r(\theta_k) = \left[\sum_{p=0}^{P} c_{r(P-p)} z_{rk}^{p} + c_{rp} z_{rk}^{P+p} - z_{rk}^{P}\right]$, and $z_{rk} = exp\{-j\pi sin\theta_k\}$. Similarity, $\mathbf{D}_T = diag\left(d_t(\varphi_1), \cdots, d_t(\varphi_K)\right) \in \mathbb{C}^{K\times K}$, with $d_t(\varphi_k) = \left[\sum_{p=0}^{P} c_{t(P-p)} z_{tk}^{p} + c_{tp} z_{tk}^{P+p} - z_{tk}^{P}\right]$, and $z_{tk} = exp\{-j\pi sin\varphi_k\}$. Let $\tilde{\mathbf{a}}_r(\theta_k)$ and $\tilde{\mathbf{a}}_t(\varphi_k)$ represent the k-th column of $\mathbf{A}'_R$ and $\mathbf{A}'_T$, respectively. It is obvious that the phases of $\tilde{\mathbf{a}}_r(\theta_k)$ and $\tilde{\mathbf{a}}_t(\varphi_k)$ have linear characteristics, thus the LS method is recommend for 2D angle estimation. It follows that

$$\begin{cases} \mathbf{h}_{tk} = -angle\left(\hat{\mathbf{a}}_t(\varphi_k)\right) \\ \mathbf{h}_{rk} = -angle\left(\hat{\mathbf{a}}_r(\theta_k)\right) \end{cases} \tag{19}$$

where $\hat{\mathbf{a}}_t$ and $\hat{\mathbf{a}}_r$ are the estimation of $\tilde{\mathbf{a}}_r(\theta_k)$ and $\tilde{\mathbf{a}}_r(\varphi_k)$. Scale ambiguity of the PARAFAC decomposition can be solved by normalizing the estimated phases. Then we construct the following matrices and vectors

$$\begin{cases} \mathbf{P}_1 = \begin{bmatrix} 1 & 1 & \cdots & 1 \\ 0 & \pi & \cdots & (\bar{M}-1)\pi \end{bmatrix}^T, \mathbf{u}_k = \begin{bmatrix} u_{k1} \\ u_{k2} \end{bmatrix} \\ \mathbf{P}_2 = \begin{bmatrix} 1 & 1 & \cdots & 1 \\ 0 & \pi & \cdots & (\bar{N}-1)\pi \end{bmatrix}^T, \mathbf{v}_k = \begin{bmatrix} v_{k1} \\ v_{k2} \end{bmatrix} \end{cases} \tag{20}$$

The solution to LS fitting for $\mathbf{u}_k$ and $\mathbf{v}_k$ are known as $\mathbf{u}_k = \mathbf{P}_1^{\dagger}\mathbf{h}_{tk}$ and $\mathbf{v}_k = \mathbf{P}_2^{\dagger}\mathbf{h}_{rk}$. Thereafter, the DOD and DOA of the k-th target can be estimated and paired via

$$\begin{cases} \hat{\varphi}_k = \arcsin\left(u_{k,2}\right) \\ \hat{\theta}_k = \arcsin\left(v_{k,2}\right) \end{cases} \tag{21}$$

Remark 2. The methods in [20] and [21] are based on SVD of the decoupling data $\mathbf{X}1 = (\mathbf{P}_R \otimes \mathbf{P}_T)\mathbf{X}$, which means only the data from the middle subarray is utilized for direction matrices estimation. In the presented algorithm, the coupled direction matrices are obtained with data from the whole array, which enables a more robust and accurate direction matrices estimation. The HOSVD, as well as the PARAFAC decomposition, can be regarded as the 'Trucker 3' model [30], which has a long history in tensor analysis. In contrast to subspace-based approaches, tensor algebra can make full use of the grid structure inherent in the data. The truncated HOSVD is not optimal in terms of giving the best fit as measured by the norm of the difference [31], but it is a good starting point for the TALS algorithm. From this point of view, the proposed PARAFAC decomposition algorithm outperforms the HOSVD method.

Remark 3. According to Theorem 1, $\mathbf{A}_R$ and $\mathbf{A}_T$ share the same column ambiguity (the same permutation matrix $\mathbf{\Pi}$), therefore the estimated angles are automatically paired.

Remark 4. It is worth noting that matrix $\mathbf{S}$ contains Doppler frequency information of the targets, which can be obtained when PARAFAC decomposition is finished. Thus Doppler frequency estimation can also be achieved by utilizing the LS method.

Remark 5. In this paper, the decoupling matrices $\mathbf{P}_R$ and $\mathbf{P}_T$ select a part the data from the estimated direction matrices, the residual data still contain angle information of the targets. However, these data have been neglected in the proposed method. More intelligent methods should be developed to further improve the accuracy of angle estimation.

3.3. Mutual coupling parameter estimation

Angle estimation accuracy would be improved if the arrays have been accurate calibrated. As the mutual coupling matrices $\mathbf{C}_R$ and $\mathbf{C}_T$ are full-rank matrices, once the mutual coupling coefficients have been estimated, the mutual coupling effect can be compensated. In what follows, the method for mutual coupling coefficients estimation is present.

Theorem 2 *([32]). For any $M \times 1$ complex vector $\mathbf{b}$ and any $M \times M$ banded complex symmetric Toeplitz matrix $\mathbf{T} = \text{toeplitz}[\mathbf{c}, 0, \ldots, 0]$, there exists*

$$\mathbf{T}\mathbf{b} = (\mathbf{Q}_1 + \mathbf{Q}_2)\mathbf{c} \tag{22}$$

where $\mathbf{c} = [c_0, \cdots, c_P]$ is a $(P+1) \times 1$ vector consisted with nonzero elements. $\mathbf{Q}_1, \mathbf{Q}_2 \in \mathbb{C}^{M\times(P+1)}$ are constructed as following

$$\begin{cases} \mathbf{Q}_1(m,p) = \begin{cases} \mathbf{b}(m+p-1), & m+p \le M+1 \\ 0, & otherwise \end{cases} \\ \mathbf{Q}_2(m,p) = \begin{cases} \mathbf{b}(m-p+1), & m \ge p \ge 2 \\ 0, & otherwise \end{cases} \end{cases} \tag{23}$$

According to Theorem 2, we have

$$\begin{cases} \mathbf{a}_t(\varphi_k) = \mathbf{C}_T\bar{\mathbf{a}}_t(\varphi_k) = [\mathbf{Q}_{t1}(\varphi_k) + \mathbf{Q}_{t2}(\varphi_k)]\mathbf{c}_t \\ \mathbf{a}_r(\theta_k) = \mathbf{C}_R\bar{\mathbf{a}}_r(\theta_k) = [\mathbf{Q}_{r1}(\theta_k) + \mathbf{Q}_{r2}(\theta_k)]\mathbf{c}_r \end{cases} \tag{24}$$

where $\mathbf{Q}_{t1}(\varphi_k)$, $\mathbf{Q}_{t2}(\varphi_k)$, $\mathbf{Q}_{r1}(\phi_k)$, $\mathbf{Q}_{r1}(\phi_k)$ are constructed according to Eq. (23). Defining $\mathbf{Q}_{tk} = \mathbf{Q}_{t1}(\varphi_k) + \mathbf{Q}_{t2}(\varphi_k)$, $\mathbf{Q}_{rk} = \mathbf{Q}_{r1}(\theta_k) + \mathbf{Q}_{r2}(\theta_k)$, with the property of Kronecker product, the k-th coupled steering vector can be recast as

$$\mathbf{a}(\theta_k, \varphi_k) = (\mathbf{Q}_{rk} \otimes \mathbf{Q}_{tk})(\mathbf{c}_r \otimes \mathbf{c}_t) = \mathbf{Q}_k\mathbf{c} \tag{25}$$

where $\mathbf{c} = \mathbf{c}_r \otimes \mathbf{c}_t$, $\mathbf{Q}_k = \mathbf{Q}_{rk} \otimes \mathbf{Q}_{tk}$ is a full column rank matrix and uncorrelated with $\mathbf{c}$. Let $\mathbf{E}_s = \hat{\mathbf{A}}_R \odot \hat{\mathbf{A}}_T$, and $\mathbf{E}_n = \mathbf{I} - \mathbf{U}_o\mathbf{U}_o$, where $\mathbf{U}_o$ is the orthogonal basis of $\mathbf{E}_s$. According to the MUSIC method,

Table 1
Comparison of the complexity.

Method	Computation load for angle estimation
ESPRIT	$\bar{M}^2\bar{N}^2L+2\left(\bar{M}-1\right)\bar{N}K^2+2\left(\bar{N}-1\right)\bar{M}K^2+3O\left(K^3\right)+O\left(\bar{M}^3\bar{N}^3\right)$
HOSVD	$\bar{M}^2\bar{N}^2K+0.5\left(\bar{M}-1\right)\bar{N}K^2+0.5\left(\bar{N}-1\right)\bar{M}K^2+O\left(K^3\right)+0.75O\left(\bar{M}^3\bar{N}^3\right)$
Proposed	$l\left[3K^3+3MNLK+\left(2K^2+K\right)(ML+NL+MN)\right]+2K\bar{M}+2K\bar{N}$

the space spanned by the columns of $\mathbf{A}$ is identical to the space spanned by $\mathbf{E}_s$. Therefore, $\mathbf{A}$ is orthogonal to the space spanned by $\mathbf{E}_n$, i.e., $\mathbf{E}_n^H\mathbf{A}=\mathbf{0}$. Hence we can obtain the following solution

$$\begin{aligned}\mathbf{c}&=arg\min_{\mathbf{c}}\sum_{k=1}^{K}\|\mathbf{E}_n\mathbf{a}(\theta_k,\varphi_k)\|^2\\&=arg\min_{\mathbf{c}}\sum_{k=1}^{K}\left\|\mathbf{E}_n^H\mathbf{Q}_k\mathbf{c}\right\|^2=\mathbf{c}^H\mathbf{Q}_n\mathbf{c}\end{aligned}\tag{26}$$

where $\mathbf{Q}_n=\sum_{k=1}^{K}\mathbf{Q}_k^H\mathbf{E}_n\mathbf{E}_n^H\mathbf{Q}_k$. According to (26), the estimate $\hat{\mathbf{c}}$ of $\mathbf{c}$ can be obtained from the eigenvector corresponding to the minimum eigenvalue of $\mathbf{Q}_n$. After normalizing $\hat{\mathbf{c}}(1)=1$, we have

$$\begin{cases}c_{tp}=\mathbf{c}(p+1)\\c_{rp}=\mathbf{c}(pP+p+1))\end{cases},p=0,\ldots,P\tag{27}$$

Up to now, we have presented the scheme for joint angle and mutual coupling estimation in bistatic MIMO radar. The major algorithmic steps of the proposed method are shown as follows:
step.1 Stake the received data into a third-order tensor $\mathcal{X}$ as Eq. (6);
step.2 Estimate the coupled matrices $\hat{\mathbf{A}}_R$ and $\hat{\mathbf{A}}_T$ through PARAFAC decomposition;
step.3 Obtain $\mathbf{A}_R'$ and $\mathbf{A}_T'$ via Eq. (18), and get the estimations of DODs and DOAs subject to LS fitting via Eq. (19)–Eq. (21);
step.4 Construct $\mathbf{E}_n$ with $\hat{\mathbf{A}}_R$ and $\hat{\mathbf{A}}_T$, then calculate $\mathbf{Q}_n$. Performing eigenvalue decomposition of $\mathbf{Q}_n$ to get $\hat{\mathbf{c}}$, and estimate the mutual coupling parameters.

4. Algorithm analysis

4.1. Identifiability analysis

Reference [4] gives the maximum parameter identifiability of the subspace based algorithm. As the transmit (receive) array geometry is a continuous subset of the receive (transmit) array in ULA based bistatic MIMO radar, the maximum identifiability of the methods in [20] and [21] is thus $\frac{\bar{M}+\bar{N}-2}{2}$.

The formulation in Eq. (15) provides an upper bound on the identifiability of the proposed PARAFAC algorithm. If there are lots of targets without the same DOD and DOA, $\mathbf{A}_R$ and $\mathbf{A}_T$ will be full row rank, i.e., $k_{\mathbf{A}_R}=N$ and $k_{\mathbf{A}_T}=M$. When $K\le L$, the inequality in Eq. (15) can be rewritten as $M+N\le K+2$, which implies the maximum number of targets that the proposed algorithm can identify is $M+N-2$; Under the condition of $K>L$, the identifiable upper bound of the proposed algorithm is $\frac{M+N+L-2}{2}$; In sum, the proposed algorithm can achieve better estimation accuracy than [20] and [21].

4.2. Computation complexity

The computation load of the proposed method is formally evaluated as follows. The iteration of Eq. (10), Eq. (12) and Eq. (14) require $l\left[3K^3+3MNLK+\left(2K^2+K\right)(ML+NL+MN)\right]$ complex multiplications, where l denotes the number of iteration. The computational complexity in Eq. (19)–Eq. (21) is $2K\bar{M}+2K\bar{N}$. The load of computing $\mathbf{Q}_n$ is $2M^2N^2(P+1)^2+M^3N^3$, and its eigenvalue decomposition requires $O(P+1)^3$. We summarize the computational loads of the proposed method, ESPRIT [20] and HOSVD [21] in Table 1. As mutual coupling coefficients estimation is not involved in [21], we only present the complexity comparison of angle estimation. According to Table 1, the complexity of the proposed method may higher than ESPRIT and HOSVD. However, the proposed method should be more efficient than ESPRIT and HOSVD when the number of antennas is very large, which will be shown in the simulation section.

4.3. CRB analysis

In this subsection, we will derive the formulas of the CRB with respect to angle and mutual coupling estimation in a bistatic MIMO radar. For simplicity, we rewrite the signal model in Eq. (5) in a more compact form

$$\mathbf{y}_l=\left[\left(\mathbf{C}_R\bar{\mathbf{A}}_R\right)\odot\left(\mathbf{C}_T\bar{\mathbf{A}}_T\right)\right]\mathbf{s}_l+\mathbf{w}_l=\mathbf{C}\bar{\mathbf{A}}\mathbf{s}_l+\mathbf{w}_l\tag{28}$$

where $\mathbf{C}=\mathbf{C}_R\otimes\mathbf{C}_T$. We assume that the signal s_l is deterministic and the variance of the noise $\{\mathbf{w}_l\}_{l=1}^{L}$ is σ^2. Then the mean $\boldsymbol{\mu}\in\mathrm{C}^{MNL\times1}$ and the covariance matrix $\boldsymbol{\Gamma}\in\mathrm{C}^{MNL\times MNL}$ of the observed data $\mathbf{y}=\left[\mathbf{y}_1^T,\cdots,\mathbf{y}_L^T\right]^T\in\mathrm{C}^{MNL\times1}$ are given by

$$\boldsymbol{\mu}=\begin{bmatrix}\mathbf{A}\mathbf{s}_1\\\vdots\\\mathbf{A}\mathbf{s}_L\end{bmatrix}=\mathbf{H}\mathbf{R},\quad\boldsymbol{\Gamma}=\mathrm{blkdiag}\{\underbrace{\sigma^2\mathbf{I}_{MN},\cdots,\sigma^2\mathbf{I}_{MN}}_{L}\}\tag{29}$$

where $\mathbf{H}=\mathrm{blkdiag}\{\underbrace{\mathbf{A},\cdots,\mathbf{A}}_{L}\}\in\mathrm{C}^{MNL\times LK}$, $\mathbf{R}=\left[\mathbf{s}_1^T,\cdots,\mathbf{s}_L^T\right]^T\in\mathrm{C}^{LK\times1}$.
Now we define the following parameter vectors $\boldsymbol{\theta}=[\theta_1,\cdots,\theta_K]$, $\boldsymbol{\varphi}=[\varphi_1,\cdots,\varphi_K]$, $\boldsymbol{\alpha}=[\boldsymbol{\theta},\boldsymbol{\varphi}]\in\mathrm{R}^{1\times2K}$, $\boldsymbol{\beta}=[\mathrm{Re}\{\mathbf{c}_r\},\mathrm{Re}\{\mathbf{c}_t\},\mathrm{Im}\{\mathbf{c}_r\},\mathrm{Im}\{\mathbf{c}_t\}]\in\mathrm{R}^{1\times4P}$ and $\boldsymbol{\gamma}=\left[\mathrm{Re}\{\mathbf{R}^T\},\mathrm{Im}\{\mathbf{R}^T\}\right]\in\mathrm{R}^{1\times2LK}$. The whole estimation parameter vector is formulated as $\boldsymbol{\zeta}=\left[\boldsymbol{\alpha},\boldsymbol{\beta},\boldsymbol{\gamma},\sigma^2\right]^T$. According to [33], the CRB matrix for $\boldsymbol{\zeta}$ is given by the inverse of the Fisher information matrix, which can be expressed as

$$\mathrm{CRB}=\frac{\sigma^2}{2}\left[\mathrm{Re}\{\boldsymbol{\Theta}^H\boldsymbol{\Theta}\}\right]^{-1}\tag{30}$$

where $\boldsymbol{\Theta}=\left[\frac{\partial\boldsymbol{\mu}}{\partial\boldsymbol{\alpha}},\frac{\partial\boldsymbol{\mu}}{\partial\boldsymbol{\beta}},\frac{\partial\boldsymbol{\mu}}{\partial\boldsymbol{\gamma}},\frac{\partial\boldsymbol{\mu}}{\partial\sigma^2}\right]$, $\frac{\partial\boldsymbol{\mu}}{\partial\boldsymbol{\alpha}}$ represents the derivative of $\boldsymbol{\mu}$ on $\boldsymbol{\alpha}$ and similar to others. It is straightforward to obtain $\frac{\partial\boldsymbol{\mu}}{\partial\boldsymbol{\gamma}}=[\mathbf{H},j\mathbf{H}]\in\mathrm{C}^{MNL\times2LK}$, $\frac{\partial\boldsymbol{\mu}}{\partial\sigma^2}=\mathbf{0}$. We define $\frac{\partial\mathbf{a}(\theta_k,\varphi_k)}{\partial\theta_k}=\mathbf{C}\left(\frac{\partial\bar{\mathbf{a}}_r(\theta_k)}{\partial\boldsymbol{\theta}_k}\otimes\bar{\mathbf{a}}_t(\varphi_k)\right)$, $\frac{\partial\mathbf{a}(\theta_k,\varphi_k)}{\partial\varphi_k}=\mathbf{C}\left(\bar{\mathbf{a}}_r(\theta_k)\otimes\frac{\bar{\mathbf{a}}_t(\varphi_k)}{\partial\varphi_k}\right)$, $k=1,\cdots,K$. The derivative of $\boldsymbol{\mu}$ in Eq. (30) with respect to $\boldsymbol{\alpha}$ is given by $\frac{\partial\boldsymbol{\mu}}{\partial\boldsymbol{\alpha}}=\left[\frac{\partial\boldsymbol{\mu}}{\partial\boldsymbol{\theta}},\frac{\partial\boldsymbol{\mu}}{\partial\boldsymbol{\varphi}}\right]=[\boldsymbol{\Delta}_1,\boldsymbol{\Delta}_2]$ with

$$\boldsymbol{\Delta}_1=\begin{bmatrix}\left(\frac{\partial\mathbf{a}(\theta_1,\varphi_1)}{\partial\theta_1}\right)s_{1,1}&\cdots,&\left(\frac{\partial\mathbf{a}(\theta_K,\varphi_K)}{\partial\theta_K}\right)s_{K,1}\\\vdots&\ddots&\vdots\\\left(\frac{\partial\mathbf{a}(\theta_1,\varphi_1)}{\partial\theta_1}\right)s_{1,L}&\cdots,&\left(\frac{\partial\mathbf{a}(\theta_K,\varphi_K)}{\partial\theta_K}\right)s_{K,L}\end{bmatrix}\in\mathrm{C}^{MNL\times K}\tag{31}$$

and

$$\boldsymbol{\Delta}_2 = \begin{bmatrix} \left(\frac{\partial \mathbf{a}(\theta_1,\varphi_1)}{\partial \varphi_1}\right) s_{1,1} & \cdots, & \left(\frac{\partial \mathbf{a}(\theta_K,\varphi_K)}{\partial \varphi_K}\right) s_{K,1} \\ \vdots & \ddots & \vdots \\ \left(\frac{\partial \mathbf{a}(\theta_1,\varphi_1)}{\partial \varphi_1}\right) s_{1,L} & \cdots, & \left(\frac{\partial \mathbf{a}(\theta_K,\varphi_K)}{\partial \varphi_K}\right) s_{K,L} \end{bmatrix} \in \mathrm{C}^{MNL\times K} \tag{32}$$

where $s_{k,l}$ being the k-th element of $\mathbf{s}_l$. The gradient of $\boldsymbol{\mu}$ over γ is given by $\frac{\partial \boldsymbol{\mu}}{\partial \gamma} = \nabla$ with

$$\nabla = \begin{bmatrix} \frac{\partial \mathbf{C}}{\partial \mathbf{c}_{r1}}\mathbf{z}_1 & \cdots, & \frac{\partial \mathbf{C}}{\partial \mathbf{c}_{rP}}\mathbf{z}_1, & \frac{\partial \mathbf{C}}{\partial \mathbf{c}_{t1}}\mathbf{z}_1 & \cdots, & \frac{\partial \mathbf{C}}{\partial \mathbf{c}_{tP}}\mathbf{z}_1 \\ \vdots & \ddots & \vdots & \vdots & \ddots & \vdots \\ \frac{\partial \mathbf{C}}{\partial \mathbf{c}_{r1}}\mathbf{z}_L & \cdots, & \frac{\partial \mathbf{C}}{\partial \mathbf{c}_{rP}}\mathbf{z}_L, & \frac{\partial \mathbf{C}}{\partial \mathbf{c}_{t1}}\mathbf{z}_L & \cdots, & \frac{\partial \mathbf{C}}{\partial \mathbf{c}_{tP}}\mathbf{z}_L \end{bmatrix} \otimes [1,\, j] \in \mathrm{C}^{MNL\times 4P} \tag{33}$$

where $\mathbf{z}_l = \bar{\mathbf{A}}\mathbf{s}_l$, $\frac{\partial \mathbf{C}}{\partial \mathbf{c}_{rp}} = \frac{\partial \mathbf{C}_R}{\partial \mathbf{c}_{rp}} \otimes \mathbf{C}_T$ and $\frac{\partial \mathbf{C}}{\partial \mathbf{c}_{tp}} = \mathbf{C}_R \otimes \frac{\partial \mathbf{C}_T}{\partial \mathbf{c}_{tp}}$. By letting $\boldsymbol{\Delta} = [\boldsymbol{\Delta}_1, \boldsymbol{\Delta}_2] \in \mathrm{C}^{MNL\times 2K}$, we have $\frac{\partial \boldsymbol{\mu}}{\partial \xi^T} = [\boldsymbol{\Delta}, \nabla, \mathbf{H}, j\mathbf{H}, \mathbf{0}]$, which yields

$$\mathrm{Re}\{\boldsymbol{\Theta}^H\boldsymbol{\Theta}\} = \begin{bmatrix} \mathbf{J} & \mathbf{0} \\ \mathbf{0} & 0 \end{bmatrix} \tag{34}$$

where $\mathbf{J}$ is given by

$$\mathbf{J} = \mathrm{Re}\left\{ \begin{bmatrix} \boldsymbol{\Delta}^H \\ \nabla^H \\ \mathbf{H}^H \\ -j\mathbf{H}^H \end{bmatrix} [\boldsymbol{\Delta}, \nabla, \mathbf{H}, j\mathbf{H}] \right\} \tag{35}$$

Let $\mathrm{CRB}_{a,c}$ denote the part of CRB which is corresponding to the angles and mutual coupling coefficients estimation. In the following steps we will extract $\mathrm{CRB}_{a,c}$ from $\mathbf{J}$ by means of diagonalisation. Let $\mathbf{P}_\Delta = \left(\mathbf{H}^H\mathbf{H}\right)^{-1}\mathbf{H}^H\boldsymbol{\Delta} \in \mathrm{C}^{LK\times 2K}$, and let $\mathbf{P}_\nabla = \left(\mathbf{H}^H\mathbf{H}\right)^{-1}\mathbf{H}^H\nabla \in \mathrm{C}^{LK\times 4P}$. Note that $\mathbf{H}^H\mathbf{H}$ is nonsingular, both $\mathbf{P}_\nabla^{-1}$ and $\mathbf{P}_\nabla^{-1}$ are valid. Furthermore, we define a transform matrix

$$\mathbf{V} = \begin{bmatrix} \mathbf{I} & \mathbf{0} & \mathbf{0} & \mathbf{0} \\ \mathbf{0} & \mathbf{I} & \mathbf{0} & \mathbf{0} \\ -\mathrm{Re}\{\mathbf{P}_\Delta\} & -\mathrm{Re}\{\mathbf{P}_\nabla\} & \mathbf{I} & \mathbf{0} \\ -\mathrm{Im}\{\mathbf{P}_\Delta\} & -\mathrm{Im}\{\mathbf{P}_\nabla\} & \mathbf{0} & \mathbf{I} \end{bmatrix} \tag{36}$$

Consequently, we have $[\boldsymbol{\Delta}, \nabla, \mathbf{H}, j\mathbf{H}]\mathbf{V} = [(\boldsymbol{\Delta} - \mathbf{H}\mathbf{P}_\Delta), (\nabla - \mathbf{H}\mathbf{P}_\nabla), \mathbf{H}, j\mathbf{H}]$. Let $\boldsymbol{\Pi}_{\mathbf{H}}^{\perp}$ denote the orthogonal projection of $\mathbf{H}^H$ onto null space, i.e., $\boldsymbol{\Pi}_{\mathbf{H}}^{\perp} = \mathbf{I} - \mathbf{H}\left(\mathbf{H}^H\mathbf{H}\right)^{-1}\mathbf{H}^H$ and $\mathbf{H}^H\boldsymbol{\Pi}_{\mathbf{H}}^{\perp} = \mathbf{0}$. It is obvious that

$$\mathbf{V}^H\mathbf{J}\mathbf{V} = \mathrm{Re}\left\{ \begin{bmatrix} \boldsymbol{\Delta}^H\boldsymbol{\Pi}_{\mathbf{H}}^{\perp} \\ \nabla^H\boldsymbol{\Pi}_{\mathbf{H}}^{\perp} \\ \mathbf{H}^H \\ -j\mathbf{H}^H \end{bmatrix} \left[\boldsymbol{\Pi}_{\mathbf{H}}^{\perp}\boldsymbol{\Delta}, \boldsymbol{\Pi}_{\mathbf{H}}^{\perp}\nabla, \mathbf{H}, j\mathbf{H}\right] \right\}$$

$$= \mathrm{Re}\left\{ \begin{bmatrix} \boldsymbol{\Delta}^H\boldsymbol{\Pi}_{\mathbf{H}}^{\perp}\boldsymbol{\Delta} & \boldsymbol{\Delta}^H\boldsymbol{\Pi}_{\mathbf{H}}^{\perp}\nabla & \mathbf{0} & \mathbf{0} \\ \nabla^H\boldsymbol{\Pi}_{\mathbf{H}}^{\perp}\boldsymbol{\Delta} & \nabla^H\boldsymbol{\Pi}_{\mathbf{H}}^{\perp}\nabla & \mathbf{0} & \mathbf{0} \\ \mathbf{0} & \mathbf{0} & \mathbf{H}^H\mathbf{H} & j\mathbf{H}^H\mathbf{H} \\ \mathbf{0} & \mathbf{0} & -j\mathbf{H}^H\mathbf{H} & \mathbf{H}^H\mathbf{H} \end{bmatrix} \right\} \tag{37}$$

Applying the property of partitioned diagonal matrix, we get

$$\mathbf{J}^{-1} = \mathbf{V}\left(\mathbf{V}^H\mathbf{J}\mathbf{V}\right)^{-1}\mathbf{V}^T$$

$$= \begin{bmatrix} \mathbf{I} & \mathbf{0} & \mathbf{0} \\ \mathbf{0} & \mathbf{I} & \mathbf{0} \\ \times & \times & \mathbf{I} \end{bmatrix} \cdot \begin{bmatrix} \mathrm{Re}\left\{\boldsymbol{\Delta}^H\boldsymbol{\Pi}_{\mathbf{H}}^{\perp}\boldsymbol{\Delta}\right\} & \mathrm{Re}\left\{\boldsymbol{\Delta}^H\boldsymbol{\Pi}_{\mathbf{H}}^{\perp}\nabla\right\} & \mathbf{0} \\ \mathrm{Re}\left\{\nabla^H\boldsymbol{\Pi}_{\mathbf{H}}^{\perp}\boldsymbol{\Delta}\right\} & \mathrm{Re}\left\{\nabla^H\boldsymbol{\Pi}_{\mathbf{H}}^{\perp}\nabla\right\} & \mathbf{0} \\ \mathbf{0} & \mathbf{0} & \times \end{bmatrix}^{-1} \cdot \begin{bmatrix} \mathbf{I} & \mathbf{0} & \times \\ \mathbf{0} & \mathbf{I} & \times \\ \mathbf{0} & \mathbf{0} & \mathbf{I} \end{bmatrix}$$

$$= \begin{bmatrix} \mathrm{Re}\left\{\boldsymbol{\Delta}^H\boldsymbol{\Pi}_{\mathbf{H}}^{\perp}\boldsymbol{\Delta}\right\} & \mathrm{Re}\left\{\boldsymbol{\Delta}^H\boldsymbol{\Pi}_{\mathbf{H}}^{\perp}\nabla\right\} & \times \\ \mathrm{Re}\left\{\nabla^H\boldsymbol{\Pi}_{\mathbf{H}}^{\perp}\boldsymbol{\Delta}\right\} & \mathrm{Re}\left\{\nabla^H\boldsymbol{\Pi}_{\mathbf{H}}^{\perp}\nabla\right\} & \times \\ \times & \times & \times \end{bmatrix}^{-1} \tag{38}$$

where $\times$ denotes the uninteresting part in the derivation. Inserting Eq. (38) and (34) into Eq. (30). All the unaffected modes can be factored out of Eq. (30), yielding

$$\mathrm{CRB}_{a,c} = \frac{\sigma^2}{2}\begin{bmatrix} \mathrm{Re}\left\{\boldsymbol{\Delta}^H\boldsymbol{\Pi}_{\mathbf{H}}^{\perp}\boldsymbol{\Delta}\right\} & \mathrm{Re}\left\{\boldsymbol{\Delta}^H\boldsymbol{\Pi}_{\mathbf{H}}^{\perp}\nabla\right\} \\ \mathrm{Re}\left\{\nabla^H\boldsymbol{\Pi}_{\mathbf{H}}^{\perp}\boldsymbol{\Delta}\right\} & \mathrm{Re}\left\{\nabla^H\boldsymbol{\Pi}_{\mathbf{H}}^{\perp}\nabla\right\} \end{bmatrix}^{-1} \tag{39}$$

By using the method of undetermined coefficient, we can obtain the inverse of a partitioned matrix. Thus the CRB with respect to angle estimation CRB_a and mutual coupling estimation CRB_c are given separately

$$\begin{cases} \mathrm{CRB}_a = \left[\mathrm{Re}\left\{\boldsymbol{\Delta}^H\boldsymbol{\Pi}_{\mathbf{H}}^{\perp}\boldsymbol{\Delta}\right\} - \mathrm{Re}\left\{\boldsymbol{\Delta}^H\boldsymbol{\Pi}_{\mathbf{H}}^{\perp}\nabla\right\}\mathrm{Re}^{-1}\left\{\nabla^H\boldsymbol{\Pi}_{\mathbf{H}}^{\perp}\nabla\right\}\mathrm{Re}\left\{\nabla^H\boldsymbol{\Pi}_{\mathbf{H}}^{\perp}\boldsymbol{\Delta}\right\}\right]^{-1} \\ \mathrm{CRB}_c = \left[\mathrm{Re}\left\{\nabla^H\boldsymbol{\Pi}_{\mathbf{H}}^{\perp}\nabla\right\} - \mathrm{Re}\left\{\nabla^H\boldsymbol{\Pi}_{\mathbf{H}}^{\perp}\boldsymbol{\Delta}\right\}\mathrm{Re}^{-1}\left\{\boldsymbol{\Delta}^H\boldsymbol{\Pi}_{\mathbf{H}}^{\perp}\boldsymbol{\Delta}\right\}\mathrm{Re}\left\{\boldsymbol{\Delta}^H\boldsymbol{\Pi}_{\mathbf{H}}^{\perp}\nabla\right\}\right]^{-1} \end{cases} \tag{40}$$

4.4. Advantages of our algorithm

By comparing the MUSIC-based method [19], the ESPRIT-based approach [20] and the HOSVD-based scheme [21], the advantages of the proposed algorithm can be briefly summarized as follows:

(1) The proposed algorithm can achieve the estimation for automatically paired two-dimensional angles, while the methods in [19,20] and [21] require additional pairing.
(2) Angle estimation of the proposed algorithm does not require SVD or spectral peak searching and hence it has much lower complexity, while the algorithms in [19,20] and [21] need eigen-decomposition, and the method in [19] uses two global one-dimensional searching.
(3) For the performance of angle estimation, more accurate and robust direction matrices can be estimated with the proposed algorithm, great improvement can be verified in the proposed algorithm than that in [19,20] and [21].
(4) The proposed algorithm can still work even under the condition of low snapshots, which will be shown in the next section.

5. Simulation results

In this section, 1000 Monte Carlo trials are taken to evaluate the performance of the proposed estimation algorithm. Consider that the bistatic MIMO radar is configured with M transmit elements and N receive elements, and L snapshots are collected. Assume that there are $K = 3$ uncorrelated sources located at the angles $(\theta_1, \varphi_1) = (-50°, -20°)$, $(\theta_2, \varphi_2) = (50°, 20°)$, $(\theta_1, \varphi_1) = (10°, 40°)$, and Doppler shifts are $\{f_k\}_{k=1}^3 = \{200, 400, 850\}$. The signal-to-noise ratio (SNR) in the simulation is defined by $\mathrm{SNR} = 10\log_{10}\|\mathbf{X} - \mathbf{W}_S\|^2/\|\mathbf{W}_S\|^2$ [dB], where $\mathbf{X}$ and $\mathbf{W}_S$ are the matrices in Eq. (5). The root mean square error (RMSE) of the angle estimation $\mathrm{RMSE}_{(a)}$ and the RMSE of the mutual coupling coefficients estimation $\mathrm{RMSE}_{(c)}$ are used for performance evaluation, which are defined as

$$\begin{cases} \mathrm{RMSE}_{(a)} = \frac{1}{K}\sum_{k=1}^{K}\sqrt{\frac{1}{1000}\sum_{i=1}^{1000}\left\{\left(\hat{\theta}_{i,k} - \theta_k\right)^2 + \left(\hat{\varphi}_{i,k} - \varphi_k\right)^2\right\}} \\ \mathrm{RMSE}_{(c)} = \frac{1}{P}\sqrt{\frac{1}{1000}\sum_{i=1}^{1000}\left\{\frac{\|\hat{\mathbf{c}}_{ti} - \mathbf{c}_t\|_2^2}{\|\mathbf{c}_t\|_2^2} + \frac{\|\hat{\mathbf{c}}_{ri} - \mathbf{c}_r\|_2^2}{\|\mathbf{c}_r\|_2^2}\right\}} \end{cases}$$

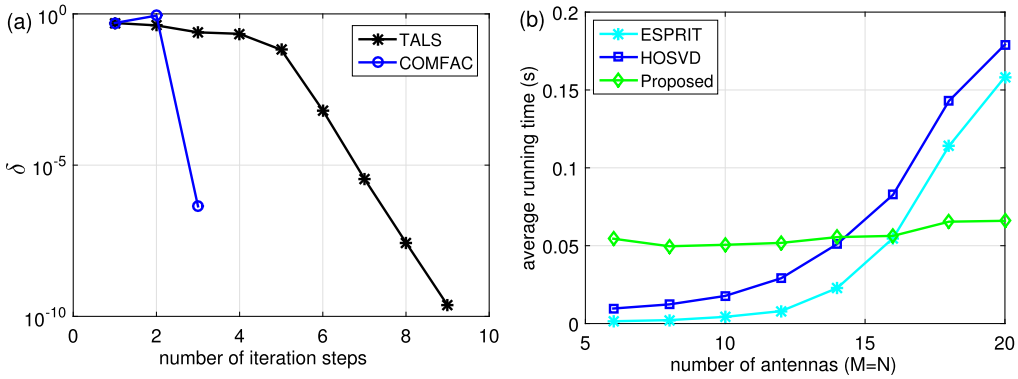

Fig. 1. Numerical results of the computational complexity: (a) convergence curve against the number of iteration steps ($M = 10$, $N = 8$, $L = 200$), (b) average running time versus number of antennas ($M = N$, $L = 200$).

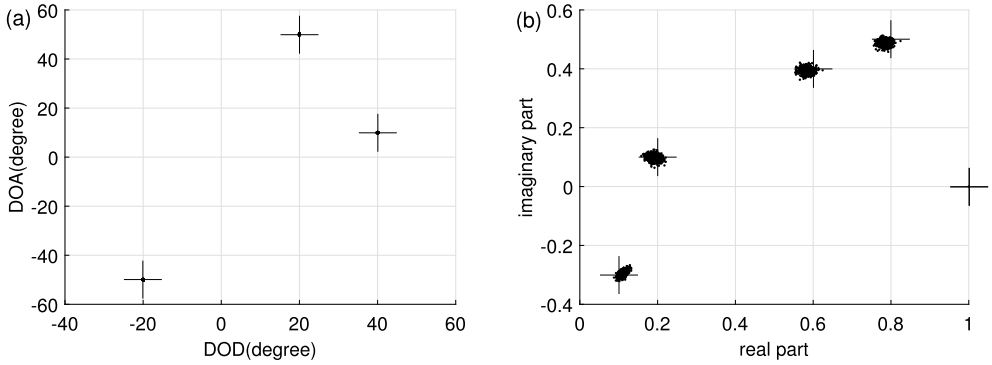

Fig. 2. Scatter results of the proposed algorithm in case (2): (a) angle estimation result, (b) mutual coupling coefficients estimation result.

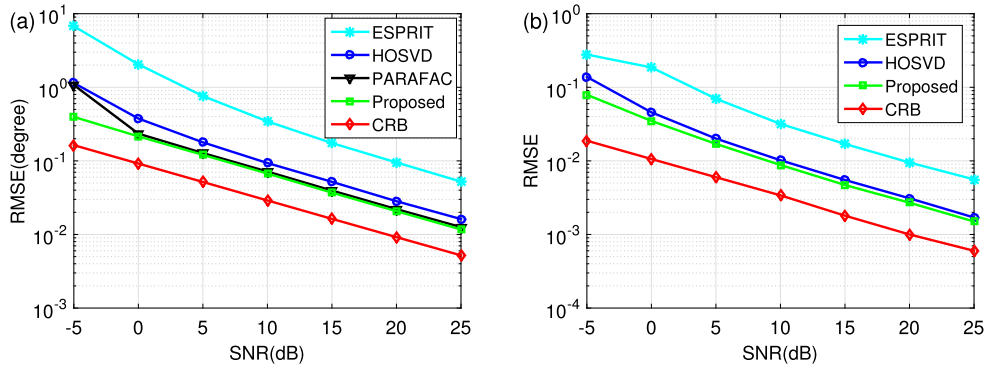

Fig. 3. Performance comparison versus SNR in case (1) with $M = 10$, $N = 8$, $L = 200$: (a) $\text{RMSE}_{(a)}$ of angle estimation versus SNR, and (b) $\text{RMSE}_{(c)}$ of mutual coupling coefficients estimation versus SNR.

where $\hat{\theta}_{i,k}$ and $\hat{\varphi}_{i,k}$, respectively, represent the estimations of θ_k and φ_k for the i th Monte Carlo trial, $\hat{\mathbf{c}}_{ri}$ and $\hat{\mathbf{c}}_{ti}$ are the observed estimates of $\mathbf{c}_r$ and $\mathbf{c}_t$ in the i th Monte Carlo trial. Two cases are considered in our simulations: (1) $P = 1$ with $\mathbf{c}_t = [1, 0.1174 + j0.0577]$, $\mathbf{c}_r = [1, -0.0121 - j0.1029]$, and (2) $P = 2$ with $\mathbf{c}_t = [1, 0.8 + j0.5, 0.2 + j0.1]$, $\mathbf{c}_r = [1, 0.6 + j0.4, 0.1 - j0.3]$.

Fig. 1 depicts the numerical results of computational complexity in case (1) with SNR = 10 dB. Fig. 1 (a) indicates that the COMFAC algorithm can converge quickly while the TALS algorithm requires more iteration steps before convergence. Fig. 1 (b) suggests that the computational loads of ESPRIT and HOSVD quickly increase with the growing antennas number. Another surprising observation is that the computational cost of the proposed method almost unchanged, which implies the proposed method is suitable for massive MIMO radar.

Fig. 2 shows the scatter results of the proposed algorithm in case (2) with $M = 10$, $N = 8$, $L = 200$, SNR = 10 dB. The estimated values and true values are denoted as solid points and cross symbols, respectively. It is explicitly shown that the angles and mutual coupling coefficients can be clearly observed.

Fig. 3 gives the $\text{RMSE}_{(a)}$ and $\text{RMSE}_{(c)}$ comparisons of different algorithms versus SNR for the case (1), and the the $\text{RMSE}_{(a)}$ and $\text{RMSE}_{(c)}$ comparison of different algorithms versus SNR in case (2) are depicted in Fig. 4. We compare our algorithm with the ESPRIT method [20], the unitary HOSVD algorithm [21], the PARAFAC approach and their CRB, where the PARAFAC approach represents the estimation algorithm that decouples before PARAFAC decomposition of the data tensor. The $\text{RMSE}_{(c)}$ performances of PARAFAC approach are between the proposed algorithm and HOSVD method and are not presented in the figures. It is indicated from Fig. 3 and Fig. 4 that RMSE performance of all the algorithms gradu-

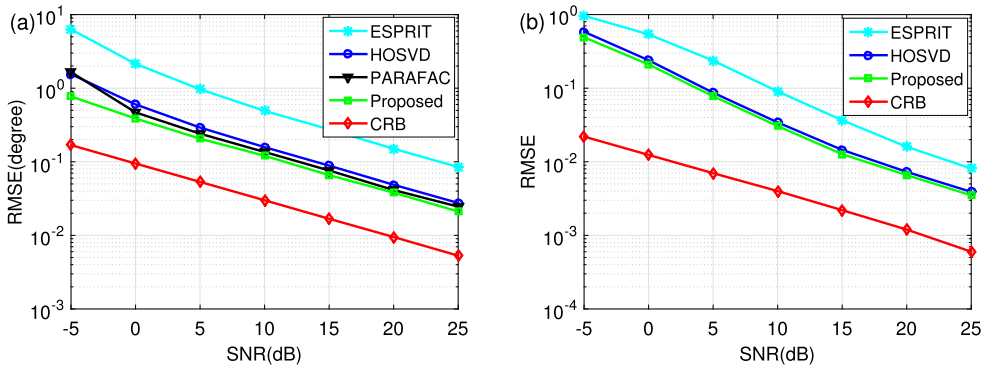

Fig. 4. Performance comparison versus SNR in case (2) with $M = 10$, $N = 8$, $L = 200$: (a) $\text{RMSE}_{(a)}$ of angle estimation versus SNR, and (b) $\text{RMSE}_{(c)}$ of mutual coupling coefficients estimation versus SNR.

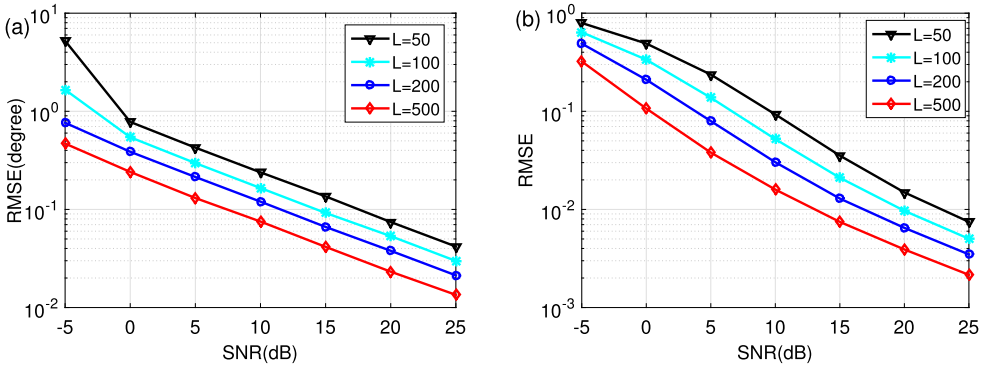

Fig. 5. RMSE performance of the proposed algorithm with different L in case (2) with $M = 10$, $N = 8$: (a) $\text{RMSE}_{(a)}$ of angle estimation versus SNR, and (b) $\text{RMSE}_{(c)}$ of mutual coupling coefficients estimation versus SNR.

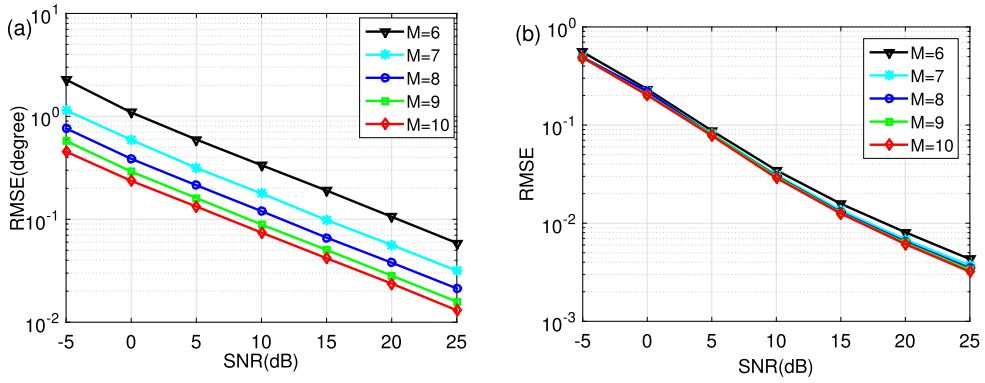

Fig. 6. RMSE performance of the proposed algorithm with different M in case (2) with $N = 8$, $L = 200$: (a) $\text{RMSE}_{(a)}$ of angle estimation versus SNR, and (b) $\text{RMSE}_{(c)}$ of mutual coupling coefficients estimation versus SNR.

ally improve with the growing SNR. Besides, larger number of the nonzero mutual coupling coefficients result in worse RMSE estimation performance. It is obvious that the PARAFAC decomposition algorithms provide better angle estimation performance than other algorithms, and the angle estimation performance of the proposed algorithm is slightly better than the PARAFAC approach, especially with low SNR environment. This improvement benefits from the fact that the proposed algorithm can achieve more robust and accurate direction matrices estimation, as elaborated in Remark 2. Thanks to the improvement in angle estimation, the proposed algorithm has slightly better $\text{RMSE}_{(c)}$ performance.

Fig. 5 illustrates the performance of the proposed algorithm in case (2) with different snapshots number L. It is clearly shown that both RMSE_a and RMSE_c decrease with snapshot number L increases. As a result, larger snapshots number L brings more accurate angle estimation with the PARAFAC model, and thanks partially to the better noise subspace estimation, the RMSE_c performance can be greatly improved.

Fig. 6 presents the RMSE performance of the proposed algorithm with different M in case (2) in the simulation. It can be seen that 2D angle estimation performance improves in collaboration with M increases, while mutual coupling coefficients estimation hardly varies. This result is consistent with theory, as M mostly contributes to the freedom of the MIMO radar, which results in accurate angle estimation, while the improvement of subspace estimation is not notable in this simulation.

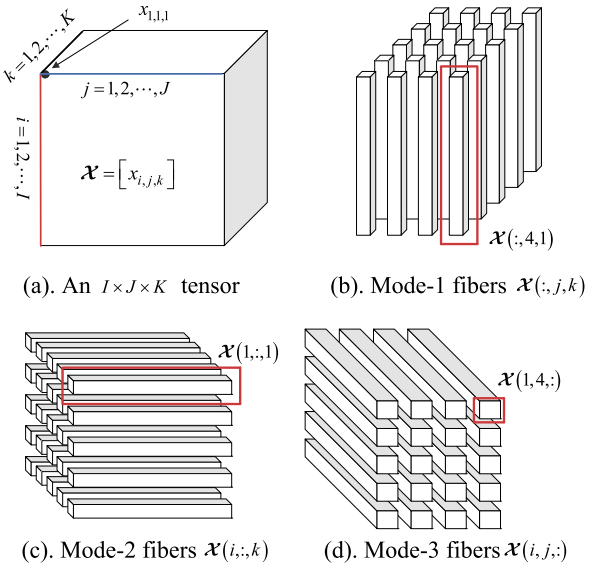

(a). An $I\times J\times K$ tensor (b). Mode-1 fibers $\mathcal{X}(:,j,k)$

(c). Mode-2 fibers $\mathcal{X}(i,:,k)$ (d). Mode-3 fibers $\mathcal{X}(i,j,:)$

Fig. 7. A third-order tensor and its fibers.

6. Conclusion

An PARAFAC decomposition algorithm is developed for joint angle and mutual coupling coefficients estimation for bistatic MIMO radar. The decoupling operation is conducted after the PARAFAC decomposition, which results in more robust and accurate directions matrices estimation. As a results, the proposed algorithm provides better angle and mutual coupling estimation performance. The proposed algorithm is attractive from the perspective of estimation accuracy as well as computation complexity. It does not require singular value decomposition of the received data while automatically pairing the estimated angles, which means it has blind and robust characteristic. Also, simulation results show the improvement of the proposed algorithm.

Acknowledgments

This work is supported by NSFC Grants (61471191, 61501233 and 61571349), the Fundamental Research Funds for the Central Universities (NP2015504), the Electronic & Information School of Yangtze University Innovation Foundation (2016-DXCX-05), and partly funded by the Priority Academic Program Development of Jiangsu Higher Education Institutions (PADA).

Appendix

The tensor operations we use are consistent with [31]. For more details about tensor algebra, we refer the reader to the review article [31].

Definition 1 *(Tensor and fibers).* A tensor is a multidimensional array. An $(I_1\times I_2\times\cdots\times I_N)$-dimensional tensor has N indices. Fibers are the higher-order analogue of matrix rows and columns. A mode-n fiber of an $(I_1\times I_2\times\cdots\times I_N)$-dimensional tensor $\mathcal{X}$ is an I_n-dimensional column vector obtained from $\mathcal{X}$ by varying the index i_n and keeping the other indices fixed. Using the MATLAB notations, $\mathcal{X}(i_1,\cdots,i_{n-1},:,i_{n+1},\cdots,i_N)$ denotes the mode-n fiber of $\mathcal{X}$ with indices $i_1,\cdots,i_{n-1},i_n+1,\cdots,i_N$. Fig. 7 illustrates a simple example of a third-order tensor and it's mode-n $(n=1,2,3)$ fibers.

Definition 2 *(Unfolding or matricization).* The unfolding operation is the process of converting the elements of a tensor to a matrix. The mode-n unfolding of a tensor $\mathcal{X}\in\mathbb{C}^{I_1\times I_2\times\cdots\times I_N}$ is denoted by $[\mathcal{X}]_{(n)}$ and arranges the mode-n fibers to be the columns of the resulting matrix. The $(i_1,i_2,\cdots,i_N)$-element of $\mathcal{X}$ maps to the (i_n,j)-th element of $[\mathcal{X}]_{(n)}$, where $j=1+\sum_{k=1,k\neq n}^{N}(i_k-1)J_k$ with $J_k=\prod_{m=1,m\neq n}^{k-1}I_m$.

For instance, if $\mathcal{X}$ is an $(4\times3\times2)$-dimensional tensor. Then three mode-n unfolding are

$$\begin{aligned}[\mathcal{X}]_{(1)}&=[\mathcal{X}(:,1,1),\mathcal{X}(:,2,1),\mathcal{X}(:,3,1),\\&\quad\mathcal{X}(:,1,2),\mathcal{X}(:,2,2),\mathcal{X}(:,3,2)]\\[\mathcal{X}]_{(2)}&=[\mathcal{X}(1,:,1),\mathcal{X}(2,:,1),\cdots,\mathcal{X}(4,:,1),\\&\quad\mathcal{X}(1,:,2),\cdots,\mathcal{X}(4,:,2)]\\[\mathcal{X}]_{(3)}&=[\mathcal{X}(1,1,:),\mathcal{X}(2,1,:),\cdots,\mathcal{X}(4,1,:),\\&\quad\mathcal{X}(1,2,:),\cdots,\mathcal{X}(4,3,:)]\end{aligned}$$

Definition 3 *(PARAFAC decomposition [34]).* The PARAFAC decomposition factorizes a tensor into a sum of component rank-one tensors. For a general Nth-order tensor $\mathcal{X}$, the PARAFAC decomposition is

$$\mathcal{X}(i_1,i_2,\cdots,i_N)=\sum_{n=1}^{N}\mathbf{A}_1(i_1,n)\cdot\mathbf{A}_2(i_2,n)\cdots\mathbf{A}_N(i_N,n)\quad(41)$$

where $\mathbf{A}_n\in\mathbb{C}^{I_n\times K}$ for $n=1,2,\cdots,N$ are called factor matrices. The PARAFAC decomposition can be written in mode-n matricized version as

$$[\mathcal{X}]_{(n)}=\mathbf{A}_n(\mathbf{A}_N\odot\mathbf{A}_{N-1}\odot\cdots\mathbf{A}_{n+1}\odot\mathbf{A}_{n-1}\odot\cdots\odot\mathbf{A}_1)^T\quad(42)$$

References

[1] S. Qin, Y.D. Zhang, M.G. Amin, DOA estimation of mixed coherent and uncorrelated targets exploiting coprime MIMO radar, Digit. Signal Process. 61 (2017) 26–34, http://dx.doi.org/10.1016/j.dsp.2016.06.006.

[2] J. Li, X. Zhang, Two-dimensional angle estimation for monostatic MIMO arbitrary array with velocity receive sensors and unknown locations, Digit. Signal Process. 24 (2014) 34–41, http://dx.doi.org/10.1016/j.dsp.2013.08.005.

[3] E. Fishler, A. Haimovich, R. Blum, D. Chizhik, L. Cimini, R. Valenzuela, MIMO radar: an idea whose time has come, in: Radar Conference, 2004, Proceedings of the IEEE, 2004, pp. 71–78.

[4] J. Li, P. Stoica, L. Xu, W. Roberts, On parameter identifiability of MIMO radar, IEEE Signal Process. Lett. 14 (12) (2007) 968–971, http://dx.doi.org/10.1109/LSP.2007.905051.

[5] G. Cui, H. Li, M. Rangaswamy, Mimo radar waveform design with constant modulus and similarity constraints, IEEE Trans. Signal Process. 62 (2) (2014) 343–353, http://dx.doi.org/10.1109/TSP.2013.2288086.

[6] H. Xie, B. Wang, F. Gao, S. Jin, A full-space spectrum-sharing strategy for massive MIMO cognitive radio systems, IEEE J. Sel. Areas Commun. 34 (10) (2016) 2537–2549, http://dx.doi.org/10.1109/JSAC.2016.2605238.

[7] A. Haimovich, R. Blum, L. Cimini, MIMO radar with widely separated antennas, IEEE Signal Process. Mag. 25 (1) (2008) 116–129, http://dx.doi.org/10.1109/MSP.2008.4408448.

[8] J. Li, P. Stoica, MIMO radar with colocated antennas, IEEE Signal Process. Mag. 24 (5) (2007) 106–114, http://dx.doi.org/10.1109/MSP.2007.904812.

[9] H. Yan, J. Li, G. Liao, Multitarget identification and localization using bistatic MIMO radar systems, EURASIP J. Adv. Signal Process. 2008 (2008) 48, http://dx.doi.org/10.1155/2008/283483.

[10] X. Zhang, L. Xu, L. Xu, D. Xu, Direction of departure (DOD) and direction of arrival (DOA) estimation in MIMO radar with reduced-dimension music, IEEE Commun. Lett. 14 (12) (2010) 1161–1163, http://dx.doi.org/10.1109/LCOMM.2010.102610.101581.

[11] C. Duofang, C. Baixiao, Q. Guodong, Angle estimation using esprit in MIMO radar, Electron. Lett. 44 (12) (2008) 770–771, http://dx.doi.org/10.1049/el:20080276.

[12] Z. Zheng, J. Zhang, Fast method for multi-target localisation in bistatic MIMO radar, Electron. Lett. 47 (2) (2011) 138–139, http://dx.doi.org/10.1049/el.2010.2577.

[13] M. Haardt, F. Roemer, G. Del Galdo, Higher-order svd-based subspace estimation to improve the parameter estimation accuracy in multidimensional harmonic retrieval problems, IEEE Trans. Signal Process. 56 (7) (2008) 3198–3213, http://dx.doi.org/10.1109/TSP.2008.917929.

[14] D. Nion, N. Sidiropoulos, Tensor algebra and multidimensional harmonic retrieval in signal processing for MIMO radar, IEEE Trans. Signal Process. 58 (11) (2010) 5693–5705, http://dx.doi.org/10.1109/TSP.2010.2058802.
[15] Y. Cheng, R. Yu, H. Gu, W. Su, Multi-svd based subspace estimation to improve angle estimation accuracy in bistatic MIMO radar, Signal Process. 93 (7) (2013) 2003–2009, http://dx.doi.org/10.1016/j.sigpro.2012.12.021.
[16] X. Wang, W. Wang, X. Li, J. Wang, A tensor-based subspace approach for bistatic MIMO radar in spatial colored noise, Sensors 14 (3) (2014) 3897–3907, http://dx.doi.org/10.3390/s140303897.
[17] X. Zhang, Z. Xu, L. Xu, D. Xu, Trilinear decomposition-based transmit angle and receive angle estimation for multiple-input multiple-output radar, Radar, Sonar Navigation, IET 5 (6) (2011) 626–631, http://dx.doi.org/10.1049/iet-rsn.2010.0265.
[18] J. Li, M. Zhou, Improved trilinear decomposition-based method for angle estimation in multiple-input multiple-output radar, IET Radar Sonar Navig. 7 (9) (2013) 1019–1026, http://dx.doi.org/10.1049/iet-rsn.2012.0345.
[19] X. Liu, G. Liao, Direction finding and mutual coupling estimation for bistatic MIMO radar, Signal Process. 92 (2012) 517–522, http://dx.doi.org/10.1016/j.sigpro.2011.08.017.
[20] Z. Zheng, J. Zhang, J. Zhang, Joint DOD and DOA estimation of bistatic MIMO radar in the presence of unknown mutual coupling, Signal Process. 92 (12) (2012) 3039–3048, http://dx.doi.org/10.1016/j.sigpro.2012.06.013.
[21] X. Wang, W. Wang, J. Liu, Q. Liu, B. Wang, Tensor-based real-valued subspace approach for angle estimation in bistatic MIMO radar with unknown mutual coupling, Signal Process. 116 (2015) 152–158, http://dx.doi.org/10.1016/j.sigpro.2015.03.020.
[22] B. Liao, C.S. Chan, Adaptive beamforming for uniform linear arrays with unknown mutual coupling, IEEE Antennas Wirel. Propag. Lett. 11 (2012) 464–467, http://dx.doi.org/10.1109/LAWP.2012.2196017.
[23] J. Li, X. Zhang, X. Gao, A joint scheme for angle and array gain-phase error estimation in bistatic MIMO radar, IEEE Geosci. Remote Sens. Lett. 10 (6) (2013) 1478–1482, http://dx.doi.org/10.1109/LGRS.2013.2260526.
[24] J. Li, X. Zhang, R. Cao, M. Zhou, Reduced-dimension music for angle and array gain-phase error estimation in bistatic MIMO radar, IEEE Commun. Lett. 17 (3) (2013) 443–446, http://dx.doi.org/10.1109/LCOMM.2013.012313.122113.
[25] N.D. Sidiropoulos, R. Bro, G.B. Giannakis, Parallel factor analysis in sensor array processing, IEEE Trans. Signal Process. 48 (8) (2000) 2377–2388, http://dx.doi.org/10.1109/78.852018.
[26] A. Di, Multiple source location – a matrix decomposition approach, IEEE Trans. Acoust. Speech Signal Process. 33 (5) (1985) 1086–1091, http://dx.doi.org/10.1109/TASSP.1985.1164700.
[27] S. Vorobyov, Y. Rong, N. Sidiropoulos, A. Gershman, Robust iterative fitting of multilinear models, IEEE Trans. Signal Process. 53 (8) (2005) 2678–2689, http://dx.doi.org/10.1109/TSP.2005.850343.
[28] R. Bro, N. Sidiropoulos, G. Giannakis, A fast least squares algorithm for separating trilinear mixtures, in: Int. Workshop Independent Component and Blind Signal Separation Anal, 1999, pp. 11–15.
[29] T. Jiang, N. Sidiropoulos, Kruskal's permutation lemma and the identification of CANDECOMP/PARAFAC and bilinear models with constant modulus constraints, IEEE Trans. Signal Process. 52 (9) (2004) 2625–2636, http://dx.doi.org/10.1109/TSP.2004.832022.
[30] L. De Lathauwer, B. De Moor, J. Vandewalle, A multilinear singular value decomposition, SIAM J. Matrix Anal. Appl. 21 (4) (2000) 1253–1278.
[31] T.G. Kolda, B.W. Bader, Tensor decompositions and applications, SIAM Rev. 51 (3) (2009) 455–500, http://dx.doi.org/10.1137/07070111X.
[32] B. Friedlander, A.J. Weiss, Direction finding in the presence of mutual coupling, IEEE Trans. Antennas Propag. 39 (3) (1991) 273–284, http://dx.doi.org/10.1109/8.76322.
[33] P. Stoica, A. Nehorai, Performance study of conditional and unconditional direction-of-arrival estimation, IEEE Trans. Acoust. Speech Signal Process. 38 (10) (1990) 1783–1795, http://dx.doi.org/10.1109/29.60109.
[34] H.A.L. Kiers, Towards a standardized notation and terminology in multiway analysis, J. Chemom. 14 (3) (2000) 105–122, http://dx.doi.org/10.1002/1099-128X(200005/06)14:3<105::AID-CEM582>3.0.CO;2-I.

Fangqing Wen was born in 1988. He received the B.S. degree in electronic engineering from Hubei University of Automotive Technology, Shiyan, China, 2011. From 2011 to 2013, he was pursuing the postgraduate study in College of Electronics and Information Engineering, Nanjing University of Aeronautics and Astronautics (NUAA), China. From October 2015 to April 2016, he was a visiting scholar at the University of Delaware, USA. He received the Ph.D. degree in NUAA, in 2016. Since 2016, he has been with the Electronic and Information School of Yangtze University, China, where he is currently an associate Professor. His research interests including MIMO radar, array signal processing and compressive sensing.

Xiaodong Xiong was born in 1964. In 1984 he received the B.S. degree in geophysical instrumentation engineering from Jianghan Petroleum University, Hubei, China and he began to work for the university immediately after the graduation. From 1988 to 1991, he was pursuing the postgraduate study in department of Information Physics of Nanjing University, Jiangsu, China. Since 1991, he has been working for Jianghan Petroleum University or Yangtze University, where he is currently a professor. His research interests are signal & information processing, geophysical detection & information technology.

Zijing Zhang was born in Beijing, China, in 1967. He received the B.S. and M.S. degrees in dynamics from the Harbin Institute of Technology, Harbin, China, in 1989 and 1992, respectively, and the Ph.D. degree in electrical engineering from Xidian University, Xi'an, China, in 2001. From August 2006 to December 2006, he was a visiting scholar at the University of Manchester, UK. From March 2016 to December 2016, he was a visiting scholar at the University of Delaware, USA. Since April 1992, he has been with the National Laboratory of Radar Signal Processing, Xidian University. His current research interests include radar signal processing and multirate filter banks design.